International Journal of Medical Toxicology & Forensic Medicine
2026, Volume 16, E53486

Research Paper

Automated Detection and Classification of Ocular Diseases Using Deep Neural Networks

Karthikeyan Murugesan[1*], Kanagajothi Dharumaraj[2], Yamuna Devi Kumar[3], Jayaraman Kumarappan[4], Kamal Raj Thiyagarajan[5], Vijayaganth Rangasamy[6]

1. *Department of Electrical and Electronics Engineering, SRM Institute of Science and Technology, Ramapuram, Bharathi Salai, Chennai, India.*
2. *Department of Mathematics, Vel Tech Rangarajan Dr.Sagunthala R&D Institute of Science and Technology, Old Mahabalipuram Road, Kalavakkam, Kancheepuram District, Tamil Nadu, India.*
3. *Department of Biomedical Engineering, Easwari Engineering College (Autonomous), Bharathi Salai, Ramapuram, Chennai – 600089, Tamil Nadu, India.*
4. *Birla Institute of Technology and Science, Pilani- Dubai Campus - Academic City, Dubai. United Arab Emirates.*
5. *Department of CSE, Rajarajeswari College of Engineering, Ramohalli Cross, Mysore Road, Kumbalgodu, India.*
6. *Department of Computer Science and Engineering, Madanapalle Institute of Technology & Science (MITS), Deemed to be University, Madanapalle, Annamayya District, Andhra Pradesh, India.*

Citation Murugesan K, Kanagajothi D, Devi Kumar Y, Kumarappan J, Thiyagarajan KR, Rangasamy V. Automated Detection and Classification of Ocular Diseases Using Deep Neural Networks. International Journal of Medical Toxicology and Forensic Medicine. 2026; 16:E53486.

https://doi.org/10.22037/ijmtfm.v16.53486

Article info:

Received: 17 September, 2026

Accepted: 01 October, 2026

Published: 02 November, 2026

Keywords:

Fundus image, Ocular disease, CNN, ODIR, ResNet, U-Net, AlexNet

ABSTRACT

Background: To prevent irreparable vision loss, it is critical to identify eye diseases in the earliest stages and start therapy as soon as feasible. Color fundus photography for patient screening is a practical and cost-effective technique. There is a dire need for automatic, trustworthy diagnostic algorithms that rely on color fundus images, since early-stage disease often shows few evident symptoms. Disorders such as diabetic retinopathy, glaucoma, age-related macular degeneration (AMD), myopia, hypertension, and cataract are indicated by changes in surrounding anatomical components, such as blood vessels, the optic disc, the fovea, and the macula.

Method: We propose three models to classify multi-label fundus images of ophthalmological diseases using deep learning and convolutional neural network (CNN) techniques. The Ocular Disease Intelligent Recognition (ODIR) database is used for this investigation. This database contains fundus photographs of patients' left and right eyes, broken down into eight categories.

Results: Compared with the other two models, ResNet and AlexNet, the U-Net classifier achieved an accuracy of approximately 99.3%.

Conclusion: Within the scope of this work, we propose an automatic multi-class learning framework for detecting eye diseases using a convolutional neural network (CNN). The current approach has several shortcomings that future research should address.

*** Corresponding Author:**
Karthikeyan Murugesan, PhD
Department of Electrical and Electronics Engineering, SRM Institute of Science and Technology, Ramapuram, Bharathi Salai, Chennai, India.
E-mail: *mkarthikeyanassistantprofessor@gmail.com*

Copyright © 2026 The Author(s);
This is an open-access article distributed under the terms of the Creative Commons Attribution-NonCommercial 4.0 International License (CC BY-NC 4.0: https://creativecommons.org/licenses/by-nc/4.0/), which permits unrestricted non-commercial use, distribution, and reproduction in any medium, provided the original work is properly cited.

Introduction

Early detection and treatment of eye disease is crucial to preventing blindness and enhancing quality of life. Diagnosis is still primarily dependent on physicians' knowledge and experience, and misdiagnoses lead to irreversible and permanent loss of vision in some instances, or blindness [1]. Many people have visual problems in their lifetime, and some of these are not too severe or can be treated at home; others require special treatment [2]. Fundus diseases are the major causes of blindness worldwide. Eye diseases like age-related macular degeneration (AMD), cataract, glaucoma, and diabetic retinopathy (DR) are common in the eye and a significant health problem in the world. These conditions can often cause progressive eye damage; therefore, early clinical diagnosis is crucial for preventing or minimizing sight loss. But this is not always the case, and there are not as many optometrists and ophthalmologists as there are patients who require screening. It is cumbersome and requires the examiner's special skill to perform a conventional fundus examination, which is not easily accomplished in large numbers. Environmental factors such as dust, humidity, sun, and other natural factors have also been shown to contribute to more infectious eye diseases in tropical areas [3]. Many imaging techniques are available to analyze retinal images, such as color fundus photography (CFP), fluorescein angiography, and optical coherence tomography (OCT).

An estimated 246 million people worldwide have low vision, and 39 million are blind [4]. About 2.2 billion people worldwide also have near- or far-vision impairments [5]. Eye diseases, such as AMD, can have very subtle early signs and can develop without early detection. Numerous CFP images are also obtained in clinical practice, and manual inspection requires a lot of time and effort. Many developing areas suffer from inadequate professional training, which worsens the problem. Therefore, an automatic diagnostic model is needed to help ophthalmologists and improve the efficiency and accuracy of diagnosis in the image domain. Deep learning methods have been used successfully in applications such as disease recognition [5, 6], object detection, sentiment analysis, and medical image classification. Computer vision and deep learning enable computers to recognize pathological patterns, freeing up ophthalmologists' time for diagnosis. While some published reports have shown positive results, relatively few studies have been designed to diagnose multiple eye diseases holistically [7]. Convolutional neural networks (CNNs), a very large family of deep neural networks (DNNs) [8–10], have made tremendous advances in medical imaging. In ophthalmology, CNNs are used for many tasks, such as disease classification, detection of anatomical structures, and more. Liefers et al. applied a pixel-wise classification approach to extract foveal centers from OCT images [11], and Meng et al. proposed a two-stage CNN model to detect the optic disc in CFP images [12, 13]. However, most published work is limited to a number of diseases. Hence, the primary goal of this work is to develop an automated fundus image classification system that can classify a broad spectrum of ophthalmologic disorders into various classes and label them. The diagnosis of ophthalmological diseases can be improved by integrating biomedical information, mathematical modeling, and AI. AI algorithms have revolutionized medical data management and hold promise for implementing computer-aided diagnosis (CAD) systems that could support mass screening programs for eye diseases, especially in areas with limited access to specialists. ANNs can learn complex nonlinear relationships and simulate key human pattern recognition capabilities. Deep neural networks consist of several layers and a large number of trainable parameters, enabling them to model complex patterns in medical images. However, proper classification depends on the proper design, training, and selection of model parameters. Hyperparameter tuning is required to fine-tune model parameters to optimize classification accuracy, efficiency, and generalization, which can be an iterative process [14, 15].

Several ways of classifying ocular disease have been proposed. In [16], they have introduced a two-stage CNN-based optic-disc localization method using optic-disc images. Other studies used local-extrema data in combination with long short-term memory networks to decrease false detections of DR and better analyze individual image regions [17]. These techniques improved accuracy and sensitivity for DR diagnosis by 96.6% and 96.4%, respectively, in fundus images [18] and were used to locate vessels, bright lesions, and red lesions. In addition, a hybrid optimized neural classifier was proposed that combines an ant colony-optimized feature set with a neural network (NN) classifier and achieved high accuracy (96.5%) for anomaly detection, suitable for early detection of DR and AMD [19]. Studies have also examined the use of OCT for diagnosing various retinal diseases [20]. These studies demonstrate the importance of deep learning, feature optimization, and retinal imaging in automated diagnosis of eye diseases, and the need for more comprehensive and effective multi-disease classification.

Materials and Methods

The Ocular Disease Intelligent Recognition (ODIR)

dataset was used to evaluate the investigated deep-learning models. The dataset includes paired color fundus photographs of the left and right eyes of patients, along with patient-level data on diagnostic keywords, age, and sex. The diagnostic information can be divided into the following eight categories: Normal (N), Diabetes (D), Glaucoma (G), Cataract (C), Age-related Macular Degeneration (AMD), Hypertension (H), Pathological Myopia (M), and Other abnormalities (O), as depicted in Table 1.

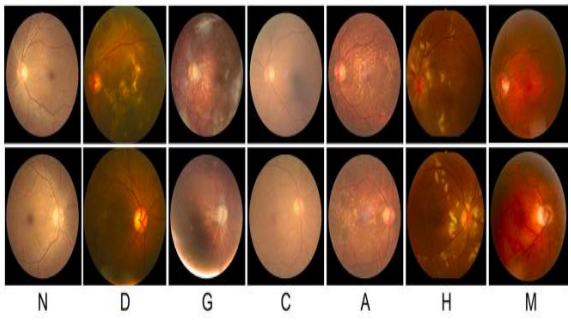
Table 1. Dataset collection (ODIR dataset).

Class	Training	Testing	Total
Normal	1135	485	1620
Diabetes	1131	485	1616
Glaucoma	207	88	307
Cataract	211	90	243
AMD	171	72	295
Hypertension	94	44	138
Myopia	177	72	249
Other abnormalities	944	402	1346

International Journal of
Medical Toxicology & Forensic Medicine

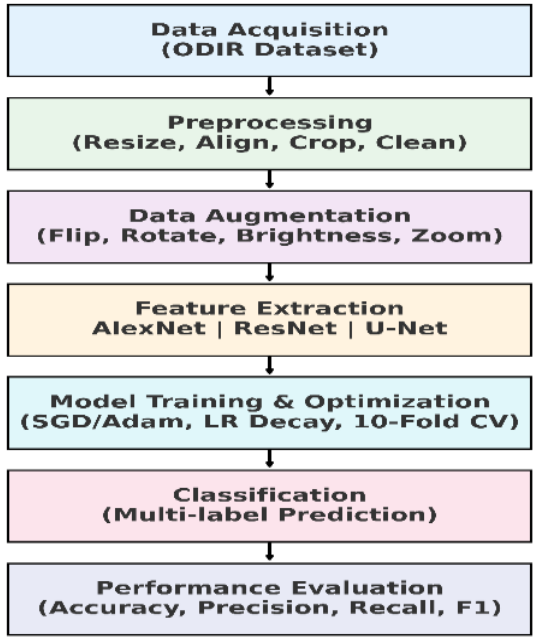
Ophthalmic diseases are inherently multi-label, as each patient can have multiple conditions affecting the eye. This means that disease frequencies are not mutually exclusive and should not be interpreted as counts of patients with each disease. To minimize ambiguity in reporting the dataset composition, the revised study explicitly distinguishes the terms patient, fundus image, and positive label occurrence. Data partitioning was carried out at the patient level, not at the image level, to avoid information leakage between paired retinal images. The grouping variable was the unique patient identifier, and both the left- and right-eye images of the same patient were kept in the same data partition. No patients provided retinal images for both the training and validation sets and the testing set. This partitioning model does not require any specific patient or specific patients and avoids having the same patients in both the development and final evaluation phases, giving a more reliable estimation of the generalization performance.

As shown in Figure 1, ODIR is a multi-class, multi-label database that contains eight different ocular disease classes. A single patient can have more than one of these diseases. The eight categories are normal (N), diabetes (D), glaucoma (G), cataract (C), age-related macular degeneration (AMD) (A), hypertension (H), myopia (M), and other diseases or abnormalities (O), as shown in Figure 2.



International Journal of
Medical Toxicology & Forensic Medicine

Figure 1. Sample Images: N- Normal, D- Diabetes, G– Glaucoma, C- Cataract, A-AMD, H– Hypertension, M-Myopia.



International Journal of
Medical Toxicology & Forensic Medicine

Figure 2. Proposed workflow for identifying the ocular disease using deep learning algorithms

Preliminary Processing: Images are resized to 128 × 128 pixels to reduce memory requirements, storage, and training time. Data augmentation is applied to address class imbalance, as some rare ocular diseases contain fewer than 10 samples compared with 401 normal images. Safe augmentation techniques increase minority-class samples, preserve labels, reduce overfitting, and improve generalization. AlexNet: AlexNet is a deep CNN consisting of five convolutional and three fully connected layers, as shown in **Figure 3**. Its first convolutional layer applies 96 filters of size 11×11×3 with a stride of four, followed by local response normalization. U-Net is an encoder-decoder architecture originally designed for biomedical image segmentation. In the current study, its hierarchical feature-learning ability was investigated to recognize ocular diseases.

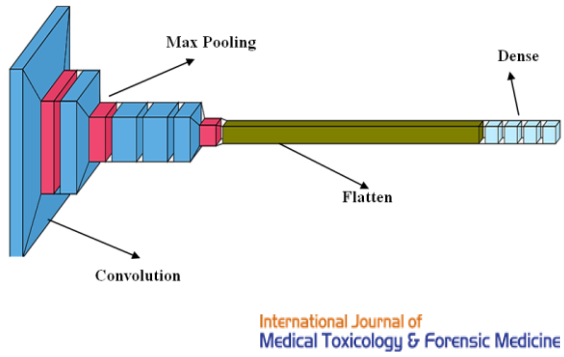


Figure 3. AlexNet's framework for detecting fake photos

The rationale for using a U-Net is that retinal structure may change in several ways, including relatively localized pathological changes or more widespread structural variations. The multi-layered convolutional structure enables the network to extract low-level information from the retina and gradually build higher-level disease concepts.

The output of the first convolutional layer is max-pooled in the first pooling layer (Max Pooling Layer 1). This pooling process uses a 3x3 filter with a stride of 2. Based on the investigation, it was found that the second convolutional layer in Convolutional Layer 2 was able to process the output of the first pooling layer. The procedure needed to be processed through 256 filters, each with dimensions 5x5x48. The number of channels is 48 because it matches the number of channels fed into it from the layer above. In this investigation, the ReLU activation function and local response normalization were used. The output of the second convolutional layer then goes to the second Max-Pooling Layer, with a stride size of 2 and a 3x3 filter.

$$Conv2 = ReLU(Convolve(MaxPool1, W2) + B2) \quad (3)$$

$$MaxPool2 = MaxPool(Conv2) \quad (4)$$

According to the findings of the research carried out, Convolutional Layer 3 is responsible for carrying out the third convolution operation. This operation calls for the application of 384 filters, each of size 256×256×256. This is the only case in which the ReLU activation function can be used.

Different ResNets are used to build our backbone CNNs so we can see how different ResNet depths affect feature extraction. Models that have already been trained on ImageNet are used to start up the backbones. As a result, the CFPs have different images. First, each CFP is scaled to 512 × 512 pixels. Next, to enhance the images for training, we randomly crop 448 by 448-pixel areas from each image. During tests, we will use it instead of center cropping. The model architecture we were given for our job consists of a ResNet-50 model and four extra layers specific to our task. Before this model was run, its weights were set. This model had already been trained on ImageNet. The input size for ResNet-50 is 100×100×3, and it uses average pooling. The refined ResNet-50 layout for transfer learning is shown in Figures 4 and 5, which illustrate the U-Net model. PyTorch is used to build each of the deep neural network systems. To conduct tests, NVIDIA GeForce 1080Ti GPUs are used. The stochastic gradient descent (SGD) approach is used to train the networks using the multi-label loss function presented in Equation (10). The learning rate initially starts at 0.007 and gradually declines over time according to the poly training rate decay policy.

We can't use the picture in our model because it's too big, so we're reshaping it by trial and error. The images are on different sides, so we used the rotate tool to align them. We cropped out the part of the eye that wasn't needed to accurately predict disease. Because each side has almost the same number of images, we used the filename as the key feature, since the other columns were less important than the image (as shown in Figures 6 and 7).

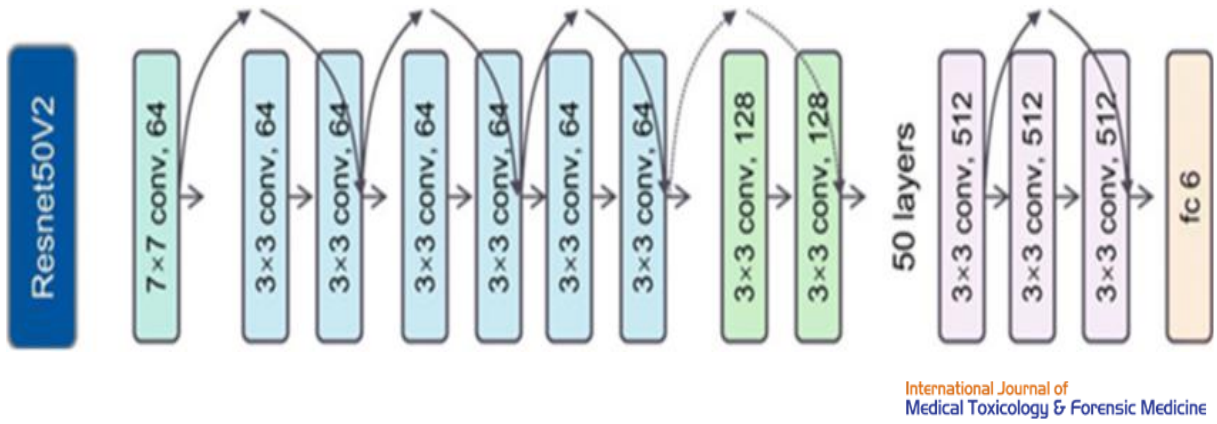
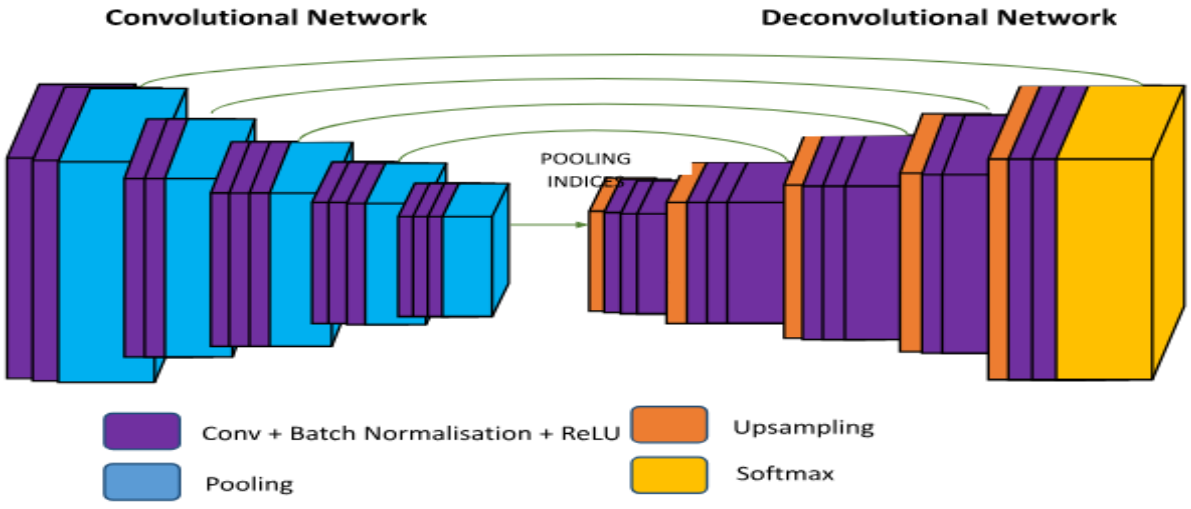
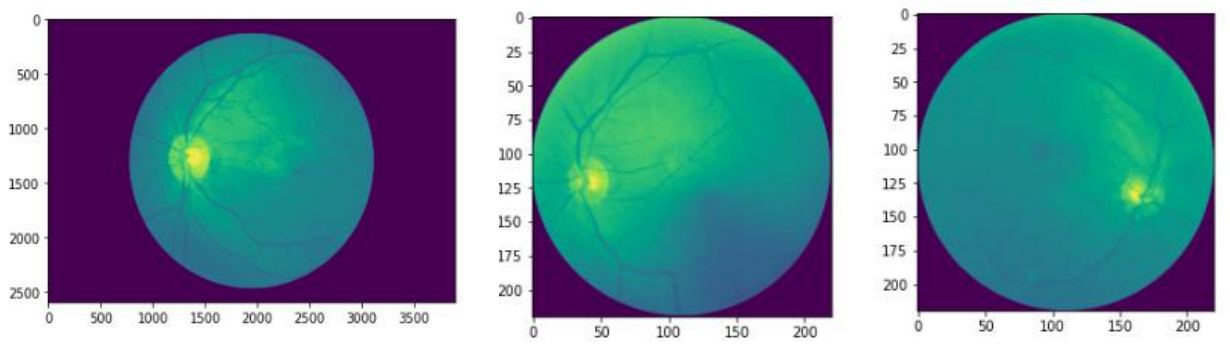


Figure 4. RESNET architecture



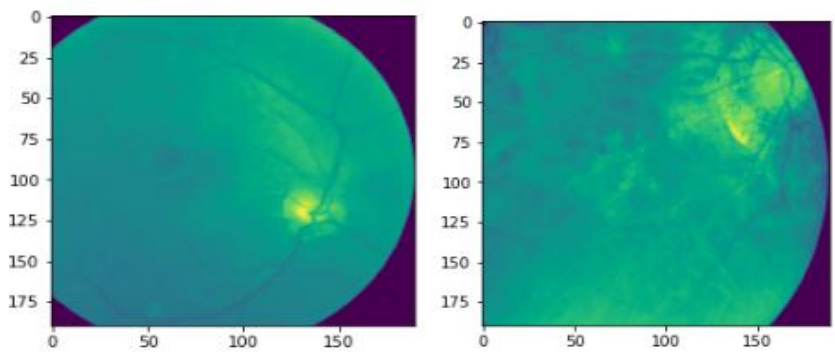
International Journal of
Medical Toxicology & Forensic Medicine

Figure 5. Architecture of the proposed U-Net



International Journal of
Medical Toxicology & Forensic Medicine

Figure 6. (a) Original Image (b) Resizing (c) Rotation



International Journal of
Medical Toxicology & Forensic Medicine

Figure 7. Cropping an image

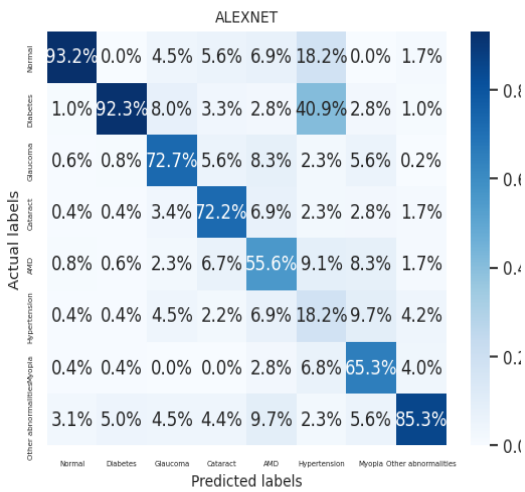
Results

All studies were conducted on a computer system with an Intel(R) Core (TM) i7-5930K CPU running at 3.50 GHz. This setup was used to run the proposed model. The machine also included a 16.0 GB NVIDIA GeForce GTX 2080 Ti graphics card. Windows 8 64-bit was the operating system that was used. The model was built using Anaconda Navigator, Python, and Jupyter Notebook 6.0.2 (Table 1).

Table 1. Specific measures of ALEXNET, RESNET and UNET.

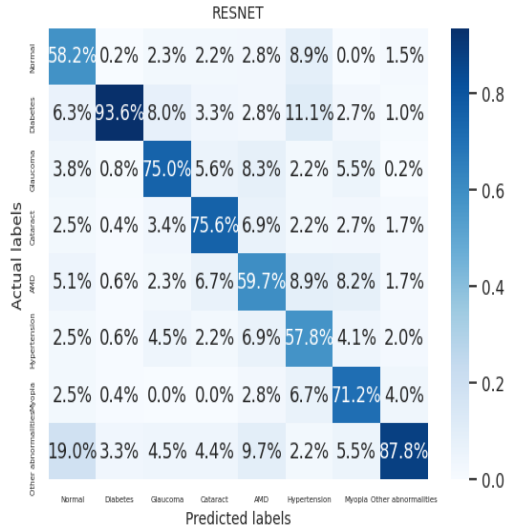
	Alexnet				Resnet				UNET			
Classes	Acc.	Prec.	Rec.	F1 score	Acc.	Prec.	Rec.	F1 score	Acc.	Prec.	Rec	F1 score
Normal	96.21%	0.93	0.93	0.93	97.15%	0.96	0.93	0.95	99.37%	0.99	0.99	0.99
Diabetes	95.29%	0.92	0.92	0.92	96.64%	0.94	0.94	0.94	99.48%	0.99	0.99	0.99
Glaucoma	97.24%	0.73	0.73	0.73	97.38%	0.73	0.75	0.74	99.48%	0.94	0.95	0.95
Cataract	97.18%	0.75	0.71	0.73	97.49%	0.76	0.76	0.76	99.31%	0.93	0.93	0.93
AMD	96.32%	0.56	0.56	0.56	96.53%	0.57	0.6	0.59	99.54%	0.94	0.94	0.94
HP	95.69%	0.17	0.18	0.18	97.38%	0.79	0.58	0.53	99.37%	0.86	0.88	0.87
Myopia	97.01%	0.64	0.65	0.64	97.38%	0.68	0.71	0.69	99.37%	0.9	0.94	0.92
Other abnormalities	93.22%	0.85	0.85	0.85	94.31%	0.87	0.88	0.88	99.37%	0.99	0.98	0.99

Figures 8-10 represent the confusion matrices for the AlexNet, ResNet, and UNet architectures.



International Journal of Medical Toxicology & Forensic Medicine

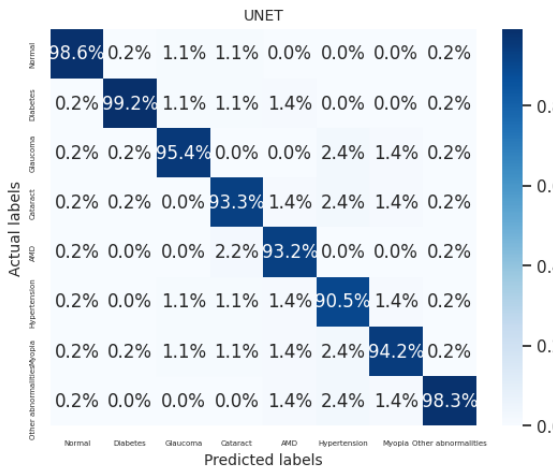
Figure 8. Confusion matrix: AlexNet



International Journal of Medical Toxicology & Forensic Medicine

Figure 9. Confusion matrix: ResNet

International Journal of Medical Toxicology & Forensic Medicine



International Journal of Medical Toxicology & Forensic Medicine

Figure 10. Confusion matrix: UNet

The accuracy comparison shows that U-Net consistently achieves superior performance across all eight ocular disease classes, reaching 99.31–99.54 percent in most categories. In contrast, AlexNet and ResNet achieve accuracies of approximately 93–97 percent, depending on disease type. The largest gain is observed in the "Other abnormalities" class, where U-Net records 99.37 percent compared to 93.22 percent (AlexNet) and 94.31 percent (ResNet), as shown in Figure 11. These results confirm U-Net's enhanced discriminative capability for multi-class ocular disease recognition.

U-Net demonstrates substantially higher precision across all disease categories, obtaining values between 0.88 and 0.99. AlexNet yields lower precision values, especially in challenging classes such as Hypertension (0.17) and AMD (0.56). ResNet shows moderate performance, with precision ranging from 0.57 to 0.96, as shown in Figure 12. U-Net's consistently higher precision indicates greater class-specific confidence and fewer false positives.

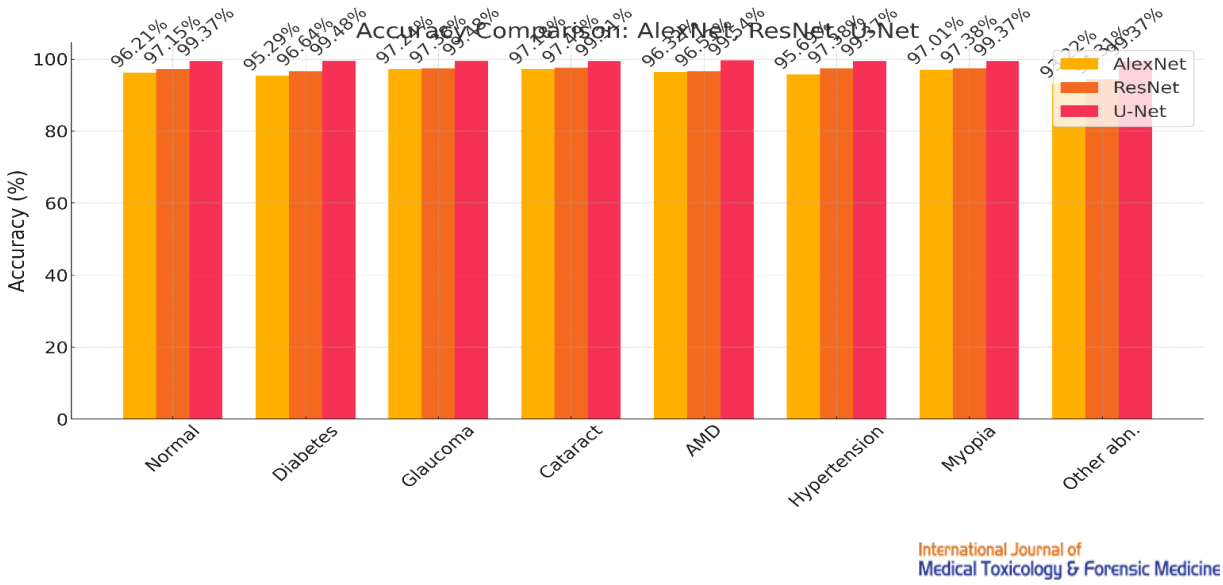


Figure 11. Accuracy comparison (AlexNet, ResNet, U-Net)

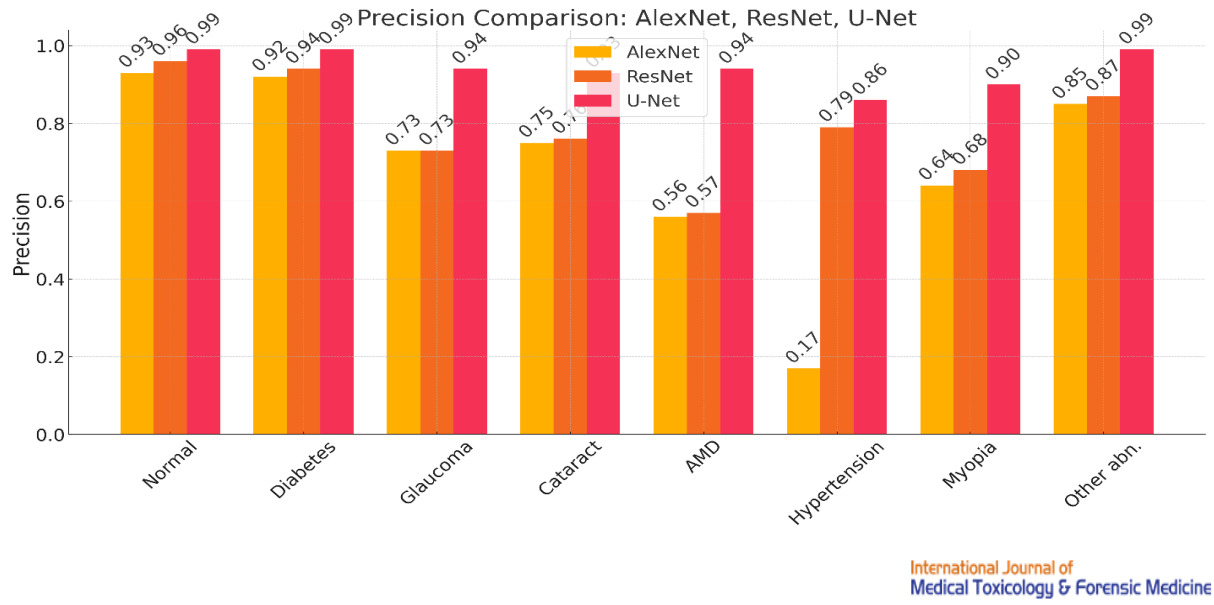


Figure 12. Precision comparison (AlexNet, ResNet, U-Net).

The recall comparison reveals U-Net's strong capability to correctly identify true positive cases, achieving recall values from 0.88 to 0.99 across all classes. AlexNet performs considerably worse, with values such as 0.18 for Hypertension and 0.56 for AMD. ResNet improves recall but remains below U-Net in all classes, as shown in Figure 13. These results show U-Net's advantage in sensitivity, especially for clinically critical categories.

U-Net maintains the highest F1-scores for all disease groups, consistently falling between 0.87 and 0.99, showing a balanced trade-off between precision and recall. AlexNet shows notable drops in complex classes such as Hypertension (0.18) and AMD (0.56), while ResNet achieves moderate performance with F1-scores between 0.53 and 0.95, as shown in Figure 14.

The macro-averaged metrics highlight U-Net's overall superiority, achieving near-perfect averages across accuracy, precision, recall, and F1-score, as shown in Figure 15. AlexNet and ResNet show considerably lower means, especially in precision and recall. This consolidated comparison strengthens U-Net's position as the most reliable model for multi-class ocular disease classification.

Figure 16 illustrates U-Net's per-class improvement relative to AlexNet and ResNet. U-Net shows significant gains across all metrics, with the largest margins in Hypertension, AMD, and abnormalities. These gains confirm that U-Net not only outperforms standard CNN baselines but also substantially enhances class-level diagnostic accuracy.

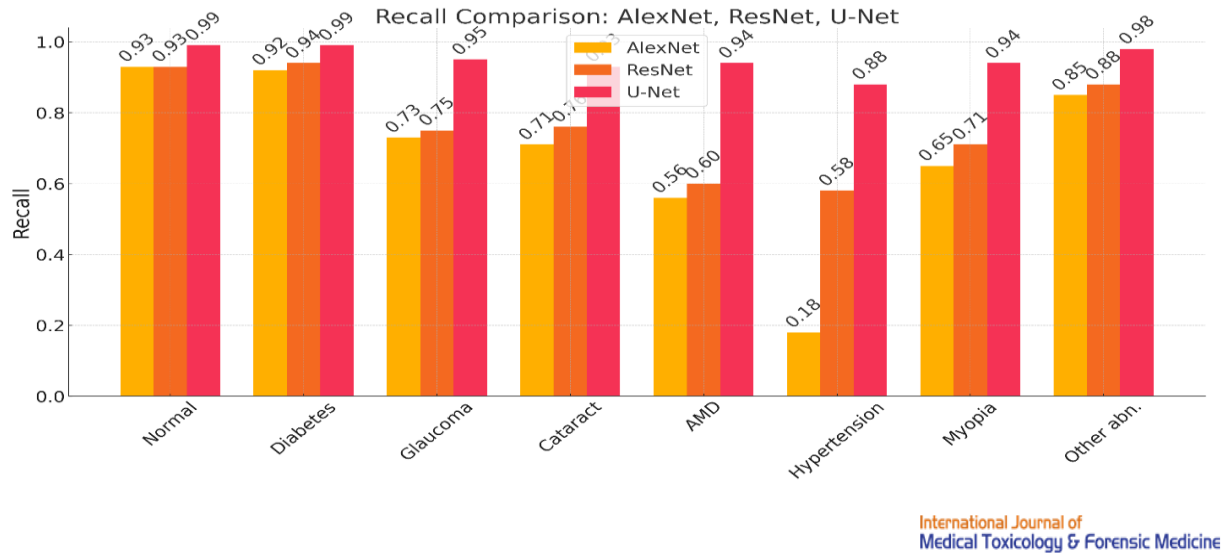


Figure 13. Recall comparison (AlexNet, ResNet, U-Net).

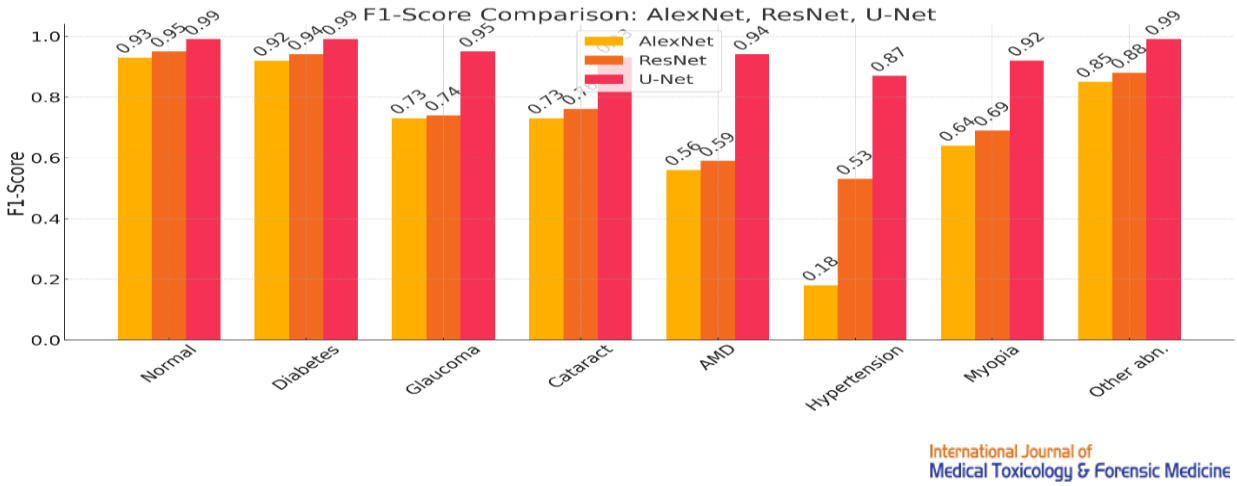


Figure 14. Score comparison (AlexNet, ResNet, U-Net).

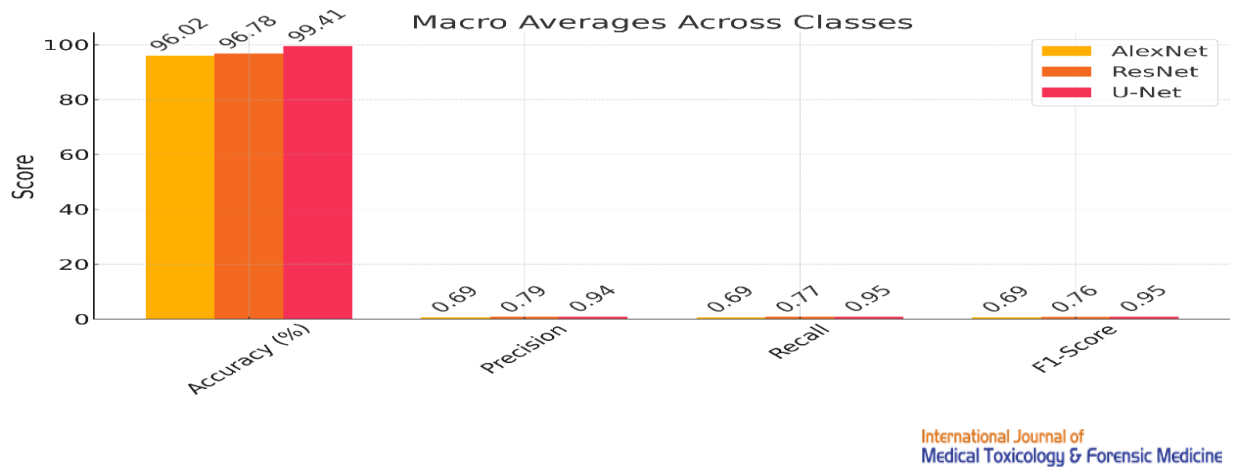


Figure 15. Macro average performance.

Discussion

Fig. 16–19 illustrate U-Net's per-class improvement relative to AlexNet and ResNet. U-Net demonstrates significant positive gains in all metrics, with the largest margins observed in Hypertension, AMD, and abnormalities. These gains verify that U-Net



Figure 16. U-Net Performance Gain Over AlexNet and ResNet.

not only outperforms but substantially enhances class-level diagnostic accuracy compared to standard CNN baselines.

Conclusion

A convolutional neural network (CNN)-based automatic multi-class learning framework for detecting ocular illnesses is proposed in this work. In real-world therapeutic settings, ophthalmological professionals most frequently use a particular retinal modality known as the fundus image. The proposed procedure implements four cutting-edge pre-trained CNN architectures and fine-tunes them using the ODIR database. Applying a transfer-learning strategy to multi-class fundus image classification is where the

originality of this work really shines through. The photographs are categorized into eight distinct categories using two distinct methodologies. Compared with the other two models, ResNet and AlexNet, which achieved accuracies of 87.13% and 84.03%, respectively, the U-Net classifier achieved an accuracy of approximately 99.3%. The current approach has several shortcomings that subsequent investigations ought to address. Because the eye ailment category labels were only given at the individual level, we could not compare the proposed approach's results with those of image-level classifiers. First, this prevented us from determining whether the proposed method outperformed other methods. Second, to keep computational complexity under control, we combined and shared the backbone CNNs used to extract features from both the left and right fundus images. Last but not least, although case numbers across categories were extremely uneven, we did not attempt to address this issue directly.

Ethical Approval

Not applicable.

Acknowledgment

None.

Funding

No external funding was received for this research.

Conflicts of Interest

The authors report there are no competing interests to declare.

References

[1] Bourne RR, Stevens GA, White RA, Smith JL, Flaxman SR, Price H, et al. Causes of vision loss worldwide, 1990–2010: a systematic analysis. Lancet Glob Health. 2013;1(6):e339–49. [DOI: 10.1016/S2214-109X(13)70113-X]

[2] WebMD Editorial Contributors. Top causes of eye problems [Internet]. WebMD; 2024 Nov 6 [cited 2026 Oct 13]. [Link]

[3] Paudel P, Ramson P, Naduvilath T, Wilson D, Phuong HT, Ho SM, et al. Prevalence of vision impairment and refractive error in school children in Ba Ria–Vung Tau province, Vietnam. Clin Exp Ophthalmol. 2014;42(3):217–26. [DOI: 10.1111/ceo.12273]

[4] World Health Organization. Blindness and vision impairment [Internet]. Geneva: World Health Organization; 2026 Feb 10 [cited 2026 Oct 13]. [Link]

[5] He J, Li C, Ye J, Qiao Y, Gu L. Self-speculation of clinical features based on knowledge distillation for accurate ocular disease classification. Biomed Signal Process Control. 2021;67:102491. [DOI: 10.1016/j.bspc.2021.102491]

[6] Alam KN, Khan MM. CNN based COVID-19 prediction from chest X-ray images. In: 2021 IEEE 12th Annual Ubiquitous Computing, Electronics & Mobile Communication Conference (UEMCON). IEEE; 2021. p. 486–92. [DOI: 10.1109/UEMCON53757.2021.9666508]

[7] Roy AG, Conjeti S, Karri SPK, Sheet D, Katouzian A, Wachinger C, et al. ReLayNet: retinal layer and fluid segmentation of macular optical coherence tomography using fully convolutional networks. Biomed Opt Express. 2017;8(8):3627–42. [DOI: 10.1364/BOE.8.003627]

[8] Litjens G, Kooi T, Bejnordi BE, Setio AAA, Ciompi F, Ghafoorian M, et al. A survey on deep learning in medical image analysis. Med Image Anal. 2017;42:60–88. [DOI: 10.1016/j.media.2017.07.005]

[9] Zhao W, Yang J, Sun Y, Li C, Wu W, Jin L, et al. 3D deep learning from CT scans predicts tumor invasiveness of subcentimeter pulmonary adenocarcinomas. Cancer Res. 2018;78(24):6881–9. [DOI: 10.1158/0008-5472.CAN-18-0696]

[10] Yang J, Deng H, Huang X, Ni B, Xu Y. Relational learning between multiple pulmonary nodules via deep set attention transformers. In: 2020 IEEE 17th International Symposium on Biomedical Imaging (ISBI). IEEE; 2020. p. 1875–8. [DOI: 10.1109/ISBI45749.2020.9098722]

[11] Liefers B, Venhuizen FG, Schreur V, van Ginneken B, Hoyng C, Fauser S, et al. Automatic detection of the foveal center in optical coherence tomography. Biomed Opt Express. 2017;8(11):5160–78. [DOI: 10.1364/BOE.8.005160]

[12] Meng X, Xi X, Yang L, Zhang G, Yin Y, Chen

X. Fast and effective optic disk localization based on convolutional neural network. Neurocomputing. 2018;312:285–95. [DOI: 10.1016/j.neucom.2018.05.114]

[13] Katibeh M, Pakravan M, Yaseri M, Pakbin M, Soleimanizad R. Prevalence and causes of visual impairment and blindness in central Iran; the Yazd eye study. J Ophthalmic Vis Res. 2015;10(3):279–85. [DOI: 10.4103/2008-322X.170362]

[14] Wang W. Further results on mean-square exponential input-to-state stability of stochastic delayed Cohen-Grossberg neural networks. Neural Process Lett. 2023;55:3953–65. [DOI: 10.1007/s11063-022-10974-8]

[15] Huang C, Liu B, Yang H, Cao j. Positive almost periodicity on SICNNs incorporating mixed delays and D operator. Nonlinear Anal Model Control. 2022;27(4):719–39. [DOI: 10.15388/namc.2022.27.27417]

[16] Simonyan K, Zisserman A. Very deep convolutional networks for large-scale image recognition. arXiv [Preprint]. 2014. arXiv:1409.1556. [DOI: 10.48550/arXiv.1409.1556]

[17] Ashir AM, Ibrahim S, Abdulghani M, Ibrahim AA, Anwar MS. Diabetic retinopathy detection using local extrema quantized Haralick features with long short-term memory network. Int J Biomed Imaging. 2021;2021:6618666. [DOI: 10.1155/2021/6618666]

[18] Bibi I, Mir J, Raja G. Automated detection of diabetic retinopathy in fundus images using fused features. Phys Eng Sci Med. 2020;43(4):1253–64. [DOI: 10.1007/s13246-020-00929-5]

[19] Devarajan D, Ramesh SM, Gomathy B. A metaheuristic segmentation framework for detection of retinal disorders from fundus images using a hybrid ant colony optimization [retracted article]. Soft Comput. 2020;24(17):13347–56. [DOI: 10.1007/s00500-020-04753-7]

[20] Playout C, Duval R, Cheriet F. A novel weakly supervised multitask architecture for retinal lesions segmentation on fundus images. IEEE Trans Med Imaging. 2019;38(10):2434–44. [DOI: 10.1109/TMI.2019.2906319]